Towards Optimisation of Forced Heating and Cooling Automated Infrared Thermograph

GIAN PIERO MALFENSE FIERRO[1] and MICHELE MEO[2]

[1]MTC Limited, Ansty Business Park, Coventry, CV7 9JU
[2]Department Aeronautics and Astronautics, University of Southampton, UK email: m.meo@soton.ac.uk

ABSTRACT

Arguably the two most important characteristics (other than quality of inspection) of non-destructive evaluation (NDE) methods are speed and non-contact inspection. These attributes coupled with real-time, automated, online and/or in-situ methods give an insight into what is expected of future inspection systems. Thermographic imaging methods over the years have been found to be well suited to meet some of these requirements. In this work a novel real-time low-cost automated heating and cooling thermographic system tailored for use within the Industry 4.0 paradigm is evaluated. The focus of this work was to improve damage detection and imaging by the optimisation of heating and/or cooling of components after manufacturing or during maintenance cycles. By changing the heating and cooling patterns during real-time automated inspection the thermographic process can be optimised for damage detection. A carbon fibre reinforced plastic (CFRP) composite sample with flat bottom holes (FBH) was used to evaluate the effective of changing heating and cooling patterns. The system was assessed using three heating/cooling profiles: heating only (HO), cooling only (CO) and heating and cooling (HC). The results show that heating and cooling patterns can play an important role in improving the effectiveness of thermography.

Keywords: Thermal Imaging, Forced Cooling, Thermography, Infrared Thermography, Composites, Modelling, Defects, Damage

1. INTRODUCTION

Infrared thermography (IRT) is a non-destructive evaluation (NDE) technique that can be used to detect damage in materials. IRT works by detecting differences in temperature, which can be caused by damage. IRT is a fast and accurate NDE technique that is used in many industries, including aerospace, automotive, and oil and gas. In recent years, there has been interest in using IRT to detect damage in composite materials. Composite materials are susceptible to various types of damage, such as barely visible impact damage (BVID), disbonding, and fatigue cracks. These types of damage are difficult to inspect using traditional NDE techniques. In comparison to other popular NDE techniques such as ultrasonic inspection, IRT has the main advantage of being a rapid, non-contact technique. There are many different IRT techniques split into two broad fields; passive and active thermography [1, 2]. Active thermography can be divided into several categories: optically stimulated thermography, [3-5], ultrasonic stimulated thermography [6, 7], eddy current stimulated thermography [8], microwave thermography [9] and a few others [10]. Active IRT generally focuses on heating up materials using heat lamps, ultrasound, or lasers, where damage is identified during the heating or cooling of the material. Recently, there has been a small number of works focused on active or forced cooling combined with a heating process [11, 12]. Identifying temperature differences, which can occur during heating or cooling, is the foundation of damage imaging. Recently, a few studies have looked into active or forced cooling in conjunction with heating. Forced cooling is an alternative method of evaluating materials that are sensitive to heat. When combined with heating, it can result in steeper temperature gradients, which has the potential to improve the detection capabilities of IRT techniques. This has been shown experimentally for thin samples [12]. Szymanik, Chady, and Gorący [12], proposed a static active heating and cooling IRT technique that used on halogen lamps for heating and a purpose build water-cooled Peltier module with

a fan for cooling. They found that heating followed by cooling was more effective at detecting damage than heating or cooling alone. Automation is a key factor in many industries, and any IRT method must be easily integrated into this framework. This has led to the development of IRT techniques that focus on automated (in-service/maintenance) [13-16] and real-time (during manufacturing) [17-21] inspection systems. Automation and real-time damage inspection are critical for the future of NDE techniques. This work proposes a low-cost automated heating and cooling IRT technique based on devices that provide high levels of temperature control and increased testing flexibility. The novelty of the proposed methodology is the integration of various components within an automated gantry system. Heating is controlled by heating pads, while cooling is controlled by a vortex tube. Both provide high levels of control while being common and inexpensive equipment. Low-cost IR cameras are used to complete the system. Surface temperature sensors and a feedback loop are used to control the heating pads. The vortex tube (VT) is used to control cooling by regulating the compressed air inlet pressure and outlet valve. VTs are a unique solution for forced cooling because they have no moving parts, require no refrigerant or direct electricity, and only need an input of compressed air [22-24]. They are predominantly used for spot cooling of machine tools during lathing and milling. To ensure even cooling across a narrow window matched to the size of the heating pads and field of view (FOV) of the infrared cameras, a simple nozzle was designed using computational fluid dynamics (CFD). This work provides an initial evaluation and proof of concept for a moving heat and cooling source. The system consists of four layers: a heating pad, an infrared camera 1, a vortex tube, and an infrared camera 2. The focus is on capturing the cooling phase during an infrared inspection. The gantry system automates the inspection process, and the cooling element of the developed system can be added to a manufacturing process to aid real-time inspections. The novelty, flexibility, and inspection results of the developed system are promising.

2. EXPERIMENTAL SETUP

The same experimental setup that was used by Fierro et al (2021) [1] was used to evaluate how inspection speed affects detection during real-time thermographic scanning. Fig. 1 shows the schematic for the low-cost automatic inspection system, comprising of a Heat Pad (HP – Aluminium PTC Heating Element ,80W, 150 ^{o}C), followed by the first IR camera (C1 – FLIR Lepton 3.5, resolution 160x120), then the Vortex Tube (VT – 130mm Aluminium Alloy Mini Vortex Tube), which is finally followed by the last IR camera (C2– FLIR Lepton 3.5, resolution 160x120). C1 and C2 were positioned to capture the temperature immediately after the heating and cooling cycles, respectively. A GFRP sample with flat bottom holes (FBH) was used to evaluate the effectiveness of the system. Fig. 1 (a) shows the side view of the system and relative distances between each component, with Fig. 1 (b) showing the top view and maximum width of the inspected region (65 mm). All components were attached to a gantry system allowing for a line scan of the sample. Initially, the HP was heated up to the required temperature, set at 105 ^{o}C, with the velocity of the gantry set at 3 mm/s, 5 mm/s and 7 mm/s to ensure smooth travel and enough heating/cooling of the samples. Figure 2 highlights the basic internal workings of a vortex tube. The VT is used to provide cooling to the surface of the inspected samples, which can be controlled directly by adjusting the control valve and input air pressure. Air pressure was set at 3 bar for the experiments carried out, with the control valve remaining in a fixed position. VTs usually are deployed with spot focusing nozzles, for this application a custom nozzle was designed and manufactured to ensure cooling along 65mm line. The table I shows the schematic of the composite (GFRP) plate inspected (250 mm x 150 mm x 3 mm). The composite plate has multiple flat bottom holes (FBH) with diameters (Φ in mm) and depths (d in mm) from the top surface indicated.

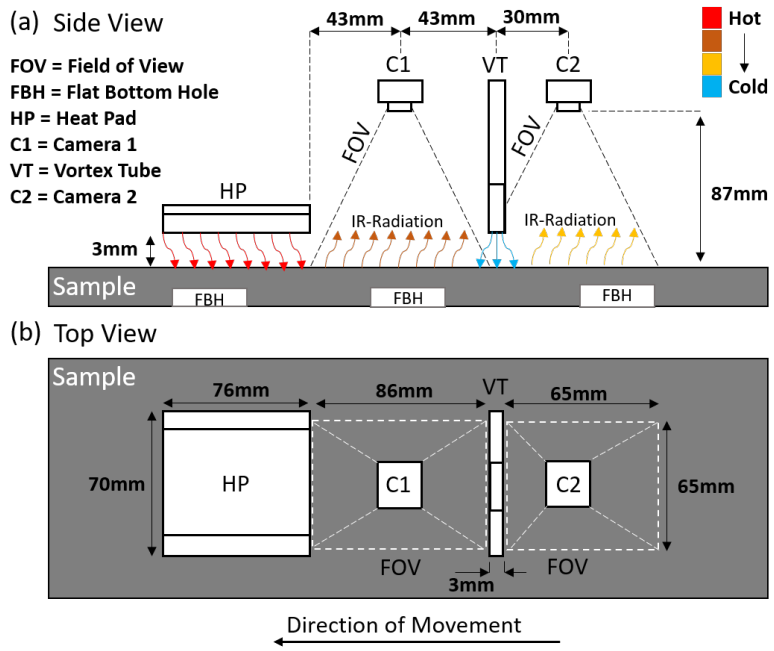

Figure 1. Schematic of experimental setup showing the side view (a) top view (b) [1]

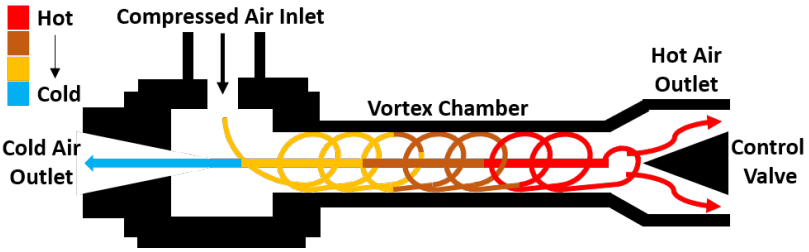

Figure 2. Illustration of basic principles of a vortex tube **[18]**

TABLE I: SUMMARY OF SAMPLE SCHEMATIC AND DIAMETER AND DEPTH OF FBH INSPECTED BY CAMERA 1 AND 2

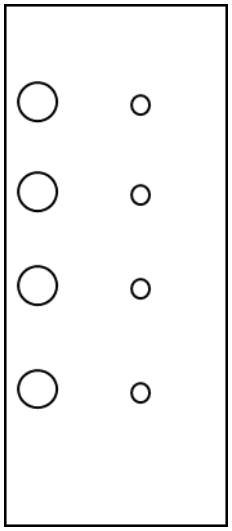

LEFT FBH	*RIGHT FBH*
Φ 3, d=1	*Φ* 1.5, d=1
Φ 3, d=1.5	*Φ* 1.5, d=1.5
Φ 3, d=2	*Φ* 1.5, d=2
Φ 3, d=2.5	*Φ* 1.5, d=2.5

3. POST-PROCESSING OF THERMAL DATA

Common processing techniques, Fourier Analysis (FA) and Principle component analysis (PCA), were used to evaluate the thermal data [26]. The focus of this work is to

evaluate the effectiveness of the speed of heating and cooling on damage detection rather than developing a new thermal image processing technique.
Data alignment was conducted as shown in Fig. 3 below. The gantry system was controlled and moved at three speeds (3 mm/s, 5 mm/s, and 7 mm/s), which required each frame to be shifted prior to processing, to ensure correct pixel is alignment. Zeros were filled into the raw data to pad and align each data point in time allowing for FA and PCA evaluation (generating the final M x N matrix). The aligned data could then be processed, providing a single image output.

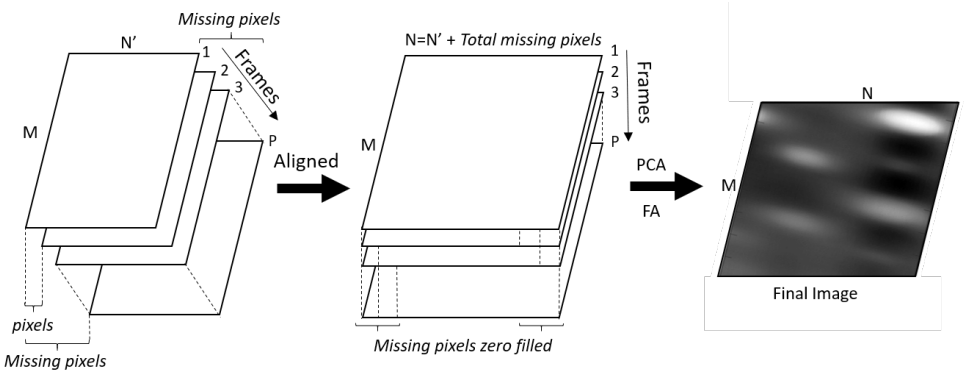

Figure 3. Data alignment for FA and PCA processing [1]

3.1. FOURIER ANALYSIS

Fourier transform converts from time domain signals to the frequency domain, this is done using the discrete Fourier transform (DFT) [27]:

$$F_n = \Delta t \sum_{k=0}^{N-1} T(k\Delta t) \exp - \frac{-j2\pi k}{N} = Re_n + Im_n \lim_{x \to \infty} \quad (1)$$

where: $j = \sqrt{-1}$ is the imaginary number, n is the frequency increment, Δt is the sampling time interval and Re and Im are the real and imaginary part of the Fourier Transform.

3.2. PRINCIPLE COMPONENT ANALYSIS (PCA)

Principle component analysis is a multivariate signal processing tool, and is a useful tool to extract signal features while filtering out noise effects by projecting the captured data onto a system of orthogonal components [28, 29]. Thermal images are captured as a three-dimensional (3D) data matrix, (A) consisting of P image frames with M x N pixels per frame (refer to Fig. 3), defined as follows:

$$A_p = \begin{bmatrix} a_{11} & \cdots & a_{1N} \\ \vdots & \ddots & \vdots \\ a_{M1} & \cdots & a_{MN} \end{bmatrix}, p = 1,2,\dots,P \quad (2)$$

Vectorisation of the 3D matrix (A_p) into a 2D vector X is done by stacking each frame as a column (P) and by combining all the vectors into a matrix X of dimension (MN x P, eq. 3):

$$x_p = (a_{11} \dots a_{M1} \dots a_{1N} \dots a_{MN})^T \quad (3)$$

$$X = (x_1, x_2, \dots, x_P) \quad (4)$$

Normalisation is commonly used to improve image results and reduce noise:

$$\hat{X} = \frac{1}{P-1}\sum_{p=1}^{P}\left(\mathrm{x}_p - \bar{\mathrm{x}}\right)\left(\mathrm{x}_p - \bar{\mathrm{x}}\right)^T \quad (5)$$

where: $\bar{\mathrm{x}} \quad = 1/P\sum_{p=1}^{P} x_p$

Finally, the singular value decomposition (SVD) is performed (eq. 6), providing the empirical orthogonal functions (EOF) which consist of the columns of matrix *U* (eq. 7). Only the first component was evaluated for this work as it contained most of the variation in the thermal data.

$$\hat{X} = \mathrm{USV}^T \quad (6)$$

$$U_i = \left(u_{1,i}, u_{2,i}, \ldots, u_{MN,i},\right)^T, i = 1,2 \quad (7)$$

4. RESULTS AND DISCUSSION

Raw thermal images were recorded for each of the three gantry speeds and then post-processed using PCA and FA to assess the performance of the heating and cooling cycle. Raw images were recorded for camera 1 and camera 2.

The results for the different speeds and cameras are summarised in Fig. 4 to Fig. 6 which show the PCA and FA images of the FBH. The PCA 1st component (Fig. 4) and 2nd component (Fig. 5) are shown for each of the speeds. The 2nd component generally shows an improvement in visualising the deeper smaller FBH when compared to the 1st component. Camera 2, which highlights the cooling phase of the inspection, emphasises the importance of the inspection speed as 5 mm/s provides the best results in terms of FBH identification. As this study, is primarily a qualitative investigation into heating, cooling and inspection speeds, further work is suggested to optimise the speed of inspection and thus the evaluation of potential defects/damage. Fig. 6 which shows the results for the Fourier analysis, identifies that the cooling phase (Camera 2) and speed of 5 mm/s allows for identification of all the FBH of the inspected GFRP sample. Speeds of 3 mm/s and 7 mm/s either allow for too much energy dissipation into the material or too little. Reinforcing the requirement to optimise inspection speed for the material being inspected. Another important factor to consider, is the defect type as this will also have an impact on the inspection capabilities. The ability of being able to control the temperature output of the system either in cooling or heating provides flexibility to assess a wide range of materials under different conditions. One of the main findings suggest that optimisation of the heating and cooling process can provide improved results. This work shows that a moving heat and cooling source can be used to provide assessment of defects in a low-cost system and can be a useful real-time inspection tool. Furthermore, the developed system can be optimised to maintain narrow temperature windows aiding in the assessment of temperature sensitive materials.

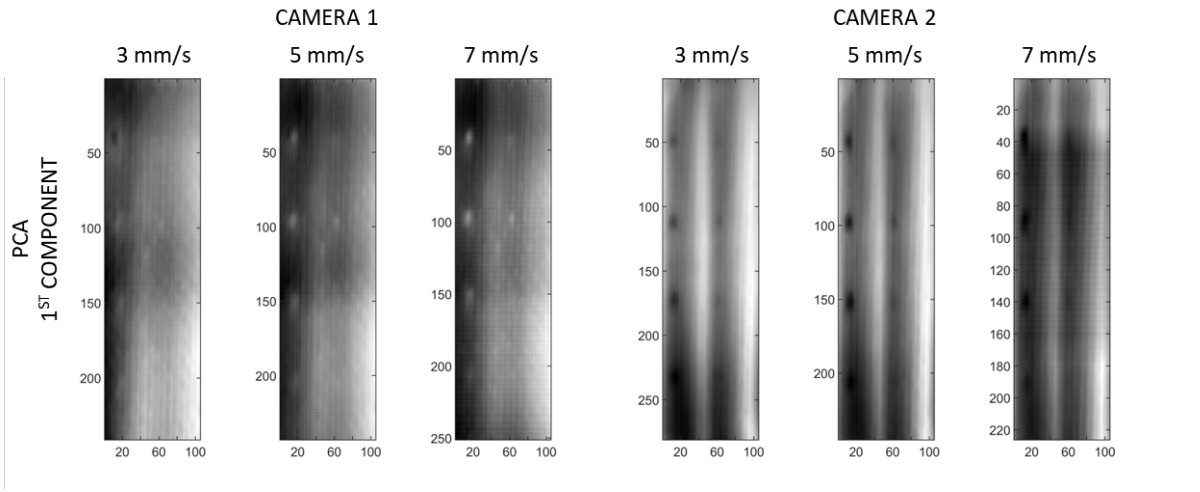

Figure 4. Camera 1 and camera 2; PCA of Camera 1 and 2, 1st PCA component.

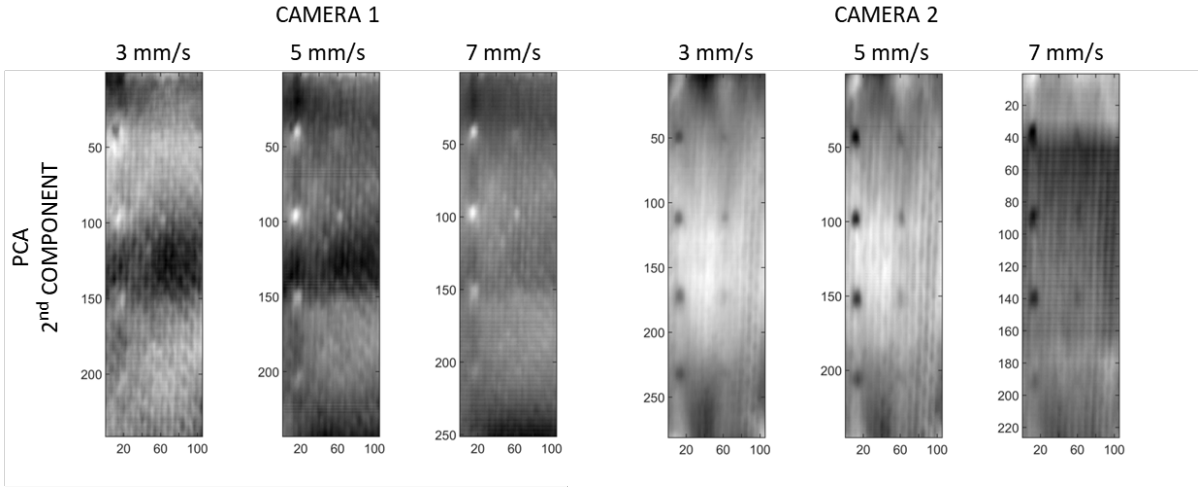

Figure 5. Camera 1 and camera 2; PCA for Camera 1 and 2, 2nd PCA component

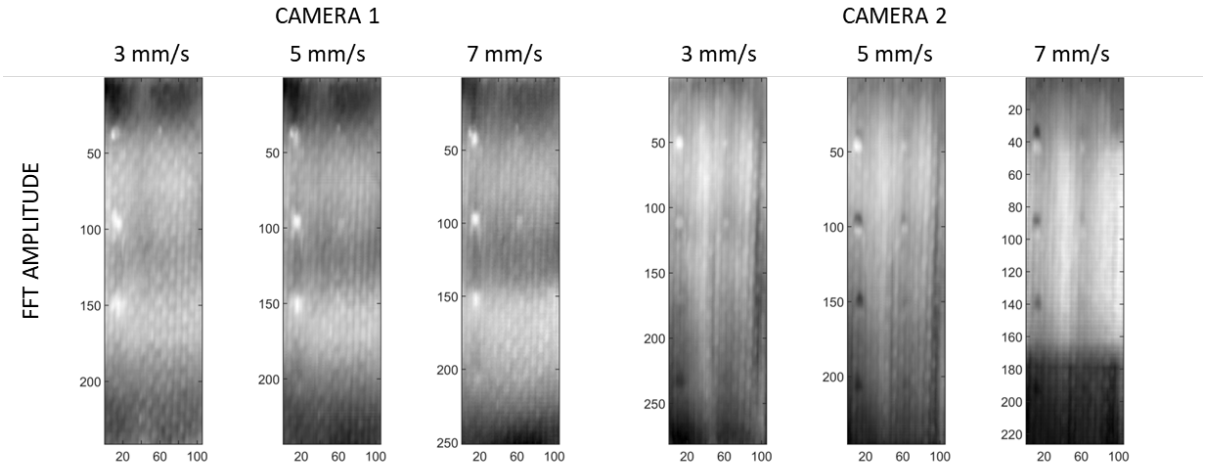

Figure 6. Camera 1 and camera 2; FA - FFT Amplitude for Camera 1 and Camera 2

5. CONCLUSION

A thermal wave imaging system combining both heating and cooling was used to evaluate FBH in a composite (GFRP) sample. The work developed a novel low-cost real-time heating and cooling thermographic system for the inspection of defects during

manufacturing or automated maintenance operations. Precise temperature control using a HP and VT accurately maintains the temperature of the inspected structure, and increases the flexibility of tailoring the system for specific inspection conditions or requirements. This research focused on a qualitative approach to evaluate three different heating and cooling scenarios to identify the potential for optimised inspection. Both PCA and FA were used to evaluate the raw thermal images and compare the different scenarios. In addition, the precise control of the heating and cooling phases provides benefits for thermally sensitive materials by reducing thermal stresses by narrowing the temperature band.

Acknowledgements

REFERENCES

[1] Ibarra-Castanedo, C., Galmiche, F., Darabi, A., Pilla, M., Klein, M., Ziadi, A., Vallerand, S., Pelletier, J.-F. and Maldague, X. P., Thermosense XXV, International Society for Optics and Photonics, pp. 450-459.(2003)

[2] Balageas, D., Maldague, X., Burleigh, D., Vavilov, V. P., Oswald-Tranta, B., Roche, J.-M., Pradere, C. and Carlomagno, G. M., Thermal (IR) and other NDT techniques for improved material inspection, *Journal of Nondestructive Evaluation* **35**, pp. 18 (2016).

[3] Maldague, X., Theory and practice of infrared technology for nondestructive testing, (2001).

[4] Bai, W. and Wong, B. S., Nondestructive Evaluation of Aging Aircraft, Airports, and Aerospace Hardware IV, International Society for Optics and Photonics, pp. 37-46.(2000)

[5] Li, T., Almond, D. P. and Rees, D. A. S., Crack imaging by scanning pulsed laser spot thermography, *NDT & E International* **44**, pp. 216-225 (2011).

[6] Zweschper, T., Riegert, G., Dillenz, A. and Busse, G., Ultrasound excited thermography-advances due to frequency modulated elastic waves, *Quantitative InfraRed Thermography Journal* **2**, pp. 65-76 (2005).

[7] Fierro, G. P. M., Ginzburg, D., Ciampa, F. and Meo, M., Imaging of Barely Visible Impact Damage on a Complex Composite Stiffened Panel Using a Nonlinear Ultrasound Stimulated Thermography Approach, *Journal of Nondestructive Evaluation* **36**, pp. 69 (2017).

[8] Wilson, J., Tian, G. Y., Abidin, I. Z., Yang, S. and Almond, D., Modelling and evaluation of eddy current stimulated thermography, *Nondestructive Testing and Evaluation* **25**, pp. 205-218 (2010).

[9] Levesque, P., Deom, A. and Balageas, D., Review of Progress in Quantitative Nondestructive Evaluation, Springer, pp. 649-654.(1993)

[10] Ciampa, F., Mahmoodi, P., Pinto, F. and Meo, M., Recent advances in active infrared thermography for non-destructive testing of aerospace components, *Sensors* **18**, pp. 609 (2018).

[11] Chady, T. and Gorący, K., AIP Conference Proceedings, AIP Publishing LLC, pp. 230025.(2018)

[12] Szymanik, B., Chady, T. and Gorący, K., Numerical modelling and experimental evaluation of the composites using active infrared thermography with forced cooling, *Quantitative InfraRed Thermography Journal* **17**, pp. 107-129 (2020).

[13] GAERTNER, M., REITINGER, B., HADERER, W., PLANK, B., KASTNER, J., GRUBER, J., MAYR, G., JAMES, V., BURGHOLZER, P. and SCHERLEITNER, E., Automated Laser Ultrasonic NDT of Carbon Fibre Reinforced Polymer Parts,

[14] Ahmadi, S., Burgholzer, P., Jung, P., Caire, G. and Ziegler, M., Super resolution laser line scanning thermography, *Optics and Lasers in Engineering* **134**, pp. 106279 (2020).

[15] Deng, B., Li, X., Wang, H., He, Y., Ciampa, F., Li, Y. and Zhou, K., Line Scanning Thermography Reconstruction Algorithm for Defects Inspection with Novel Velocity Estimation and Image Registration, *IEEE Sensors Journal*, (2020).

[16] Peng, Y., Huang, S., Deng, B., He, Y., Guo, X., Wang, H. and Han, J., Joint Scanning Electromagnetic Thermography for Industrial Motor Winding Defect Inspection and Quantitative Evaluation, *IEEE Transactions on Industrial Informatics*, (2020).

[17] Fierro, G. P. M., Flora, F. and Michele, M., 12th International Workshop on Structural Health Monitoring: Enabling Intelligent Life-Cycle Health Management for Industry Internet of Things (IIOT), IWSHM 2019, DEStech Publications Inc., pp. 2294-2301.(2019)

[18] Flora, F., Boccaccio, M., Fierro, G. and Meo, M., Real-time thermography system for composite welding: Undamaged baseline approach, *Composites Part B: Engineering*, pp. 108740 (2021).

[19] Juarez, P. D., Cramer, K. E. and Seebo, J. P., Thermosense: Thermal Infrared Applications XXXVIII, International Society for Optics and Photonics, pp. 986109.(2016)
[20] Juarez, P. D. and Gregory, E. D., AIP Conference Proceedings, AIP Publishing, pp. 120005.(2019)
[21] Yadav, N., Oswald-Tranta, B., Schledjewski, R. and Habicher, M., Thermosense: Thermal Infrared Applications XLII, International Society for Optics and Photonics, pp. 114090H.(2020)
[22] Agarwal, G., McConkey, Z. P. and Hassard, J., Optimisation of vortex tubes and the potential for use in atmospheric separation, *Journal of Physics D: Applied Physics* **54**, pp. 015502 (2020).
[23] Polihronov, J. G. and Straatman, A. G., Thermodynamics of angular propulsion in fluids, *Physical review letters* **109**, pp. 054504 (2012).
[24] Ranque, G., Experiments on expansion in a vortex with simultaneous exhaust of hot air and cold air, *J. Phys. Radium* **4**, pp. 112-114 (1933).
[25] Polihronov, J. G. and Straatman, A. G., The vortex tube effect without walls, *Canadian Journal of Physics* **93**, pp. 850-854 (2015).
[26] Wang, Z., Tian, G., Meo, M. and Ciampa, F., Image processing based quantitative damage evaluation in composites with long pulse thermography, *NDT & E International* **99**, pp. 93-104 (2018).
[27] Maldague, X. and Marinetti, S., Pulse phase infrared thermography, *Journal of Applied Physics* **79**, pp. 2694-2698 (1996).
[28] Rajic, N., Principal component thermography for flaw contrast enhancement and flaw depth characterisation in composite structures, *Composite structures* **58**, pp. 521-528 (2002).
[29] Winfree, W. P., Cramer, K. E., Zalameda, J. N., Howell, P. A. and Burke, E. R., Thermosense: Thermal Infrared Applications XXXVII, International Society for Optics and Photonics, pp. 94850S.(2015)